AN APPROACH TO THE STUDY OF TRANSVERSE MIXING IN STREAMS

László Somlyódy

August 1980
PP-80-6

INTERNATIONAL INSTITUTE FOR APPLIED SYSTEMS ANALYSIS
A-2361 Laxenburg, Austria

THE AUTHOR

László Somlyódy is a research scientist at the International Institute for Applied Systems Analysis, Schloss Laxenburg, 2361 Laxenburg, Austria and also scientific advisor for the Research Center for Water Resources Development (VITUKI), Budapest, Hungary.

ABSTRACT

Transverse mixing under steady conditions is studied by introducing the mass streamline as the streamline of the mass density vector field. No transport occurs perpendicular thereto. The mass streamline is defined by two equations, written preferably in a curvilinear set of coordinates consisting of streamlines and the trajectories perpendicular thereto. The mass streamlines and the concentration field are determined simultaneously by the method of finite differences. The former present a visual picture about the mixing process. The equations derived allow the calculation of the transverse dispersion coefficient, too, if the concentration field is given. Two methods are described, one resembling in nature the generalized change of momentum method, the other allowing the determination of the variations in D_b over the plane.

To verify the methods derived for determining the concentration field and the dispersion coefficient the results of analytical- and numerical solutions, the calculated and observed concentrations have been compared in different cases. Tracer studies have been made on five different streams ($Q = 0.25 - 2000\ m^3s^{-1}$) and data published in the literature have also been used. The limitations of the two-dimensional treatment have been examined finally.

Key words: streams, channels, hydraulics, diffusion, dispersion, turbulence, water, water pollution, numerical methods.

AN APPROACH TO THE STUDY OF TRANSVERSE MIXING IN STREAMS

by László Somlyódy

INTRODUCTION

Previous work

An understanding of the concentration distribution of pollutants discharged into the recipients, in other words of the mixing process, is of paramount importance in solving pollution control problems, in site selection of effluent discharges and water diversions, in designing freshwater-cooled power stations, as well as in planning a water quality observation network.

The description of the process involves the equations of motion, continuity and transport, the correlation between density and concentration, further the application of some kind of turbulence model. Of the latter the k-ε model developed by Launder and Spalding (9), their co-workers and followers appears most promising, in which the equations of turbulent kinetic energy and energy dissipation are used for determining the eddy viscosity coefficients. In this generalized treatment at least seven partial differential equations must be solved simultaneously, on which the scanty experience thus far available applies mostly to rather simple flow patterns.

The methods of practical interest, including the one to be presented subsequently, are greatly simplified over the foregoing general formulation. Thus assuming the effluent to be discharged with the same velocity and density as in the ambient current, the process is described solely by the equation of turbulent diffusion, whereas the quantities (velocity components and diffusion coefficients) required for the solution are entered as results obtained by some other method (field-, or laboratory measurement, empirical formulae). A solution of the equation can hereafter be attempted by a numerical method with known initial- and boundary conditions.

Of the numerical methods the one of finite differences is perhaps most widely used to such problems. Difficulties are commonly encountered when the phenomenon is influenced simultaneously by several processes of different time scales and characters (e.g. diffusion and convection in the various directions). In such cases efforts must be made besides ensuring stability and convergence, further acceptable computer time, also at minimizing the phase- and amplitude error (Verboom and Vreugdenhil (21)). This can be achieved by multi-step, special schemes, which have been analysed in detail and examined for their potential applications by several investigators including Verboom (10) and Holly (6).

In the majority of problems steady flow and pollutant discharge can be assumed. Additional simplifications are made possible by the channel geometry ($B \gg H$), as a result of which uniformity over depth occurs usually within a short distance, the process being thus reduced to one of transverse mixing.

Under the foregoing assumption we are justified in describing the phenomenon by the two-dimensional, steady-state equation of turbulent dispersion, as attempted also by Holley (4), Yotsukara and Sayre (23) and others. As demonstrated by the analytical investigations of Sayre and Chang (13) the effect of longitudinal dispersion is negligible in this case. By various considerations the equation itself can be reduced to a simplified form more readily adapted to the stream characteristics and the data available, and easier to solve numerically than those mentioned before. These have prompted Fischer to introduce the stream tube concept (3), (12), (22), Yotsukara and Cobb (21) the cumulative discharge, Chang (23), Yotsukara and Sayre (23), further Somlyódy (14) the orthogonal, curvilinear system of coordinates following the bend conditions. Further progress has been achieved by Somlyódy (16) upon introducing the streamlines of the mass density vector field $\underline{\tilde{\tilde{J}}} = \widetilde{c\,\underline{v}}$, the concept and equations of the mass streamline. A more detailed description of this approach will be given subsequently.

The coefficient of transverse mixing involved in the governing equation is in general inaccessible to theoretical determination, since it reflects the effects of both turbulence and non-uniformities over depth, and is found in the majority of cases by tracer measurements. Systematical experiments have provided the means for studying the dispersion coefficient in correlation with the principal hydraulic and geometric variables. In this respect the works of Bansal (1), Paal et al. (11), Krishnappen and Lau (7), Lau and Krishnappen (8), further of Muszkalay (10) are to be mentioned.

The estimation of the dispersion coefficient from a known concentration field may be termed an inverse problem, the solution of which becomes necessary after the completion of tracer measurements. Here again the development of a method of sufficiently general validity is considered desirable. The perhaps most frequently adopted approach is the change of moment method generalized by Holley (4), (5), (7).

Objective

The aims of the present paper are i) to derive the equations of the mass streamline in a more general way than before, and to present in details the main characteristics thereof, ii) to develop numerical methods for solving the two problems mentioned before, iii) to apply these methods on artificial and natural streams of different size and character, finally iv) to investigate the limitations of the two--dimensional approach.

GOVERNING EQUATIONS

The equation of turbulent diffusion

Under the assumptions mentioned in the foregoing the continuity equation

$$\mathrm{div}\ (h\ \underset{\sim}{\tilde{\tilde{J}}}) = 0 \qquad (1)$$

related to the mass density vector $\underset{\sim}{\tilde{\tilde{J}}} = \widetilde{\overline{c\ \underset{\sim}{v}}}$ can be written in a curvilinear, orthogonal system of coordinates (x, y) following more-or-less closely the curvatures of the stream (Fig.1) into the form

$$\frac{\partial}{\partial x}(m_y h\ \breve{\bar{v}}_x \breve{\bar{c}}) + \frac{\partial}{\partial y}(m_x h\ \tilde{\bar{v}}_y \breve{\bar{c}}) \cong \frac{\partial}{\partial y}\left(\frac{m_x}{m_y}\ h\ D_y \frac{\partial \tilde{\bar{c}}}{\partial y}\right), \qquad (2)$$

This is the familiar, two-dimensional equation of turbulent dispersion (c.f. Yotsukara and Sayre (23)). Here c is concentration, v_x and v_y are the local velocity components, D_y is the local dispersion coefficient, h the local flow depth, while m_x and m_y are the metric coefficients. The overbar above a symbol indicates averaging over time, while the wave-line a depth integrated value. The overbar will be omitted subsequently, unless it is considered essential.

The (s,b) system consisting of the streamlines and the trajectories perpendicular thereto, of the vector field $\underset{\sim}{\tilde{v}}$ is defined hereafter (Fig.1). The streamlines are described by two equations ($\tilde{v}_x \neq 0$, $\partial q/\partial y \neq 0$):

$$\frac{dy}{dx} = \frac{m_x}{m_y}\frac{\tilde{v}_y}{\tilde{v}_x} = \frac{m_x}{m_y} \tan \chi_q \tag{3}$$

and

$$\frac{dy}{dx} = -\frac{\partial q/\partial x}{\partial q/\partial y} = -\frac{1}{m_y h \tilde{v}_x}\frac{\partial}{\partial x}\int_{y_l}^{y} m_y h\, \tilde{v}_x\, dy' \tag{4}$$

indicating that i) the vector $\underline{\tilde{v}}$ is at every point the tangent of the streamline and ii) the change in the cumulative discharge $q = \int_{y_l}^{y} m_y h\, \tilde{v}_x\, dy'$ along the streamline (averaged over time and depth) is zero. In this system of coordinates the transverse convective term is logically eliminated and Eq.(2) assumes the form

$$\frac{\partial}{\partial s}(m_b\, h\, \tilde{v}_s\, \tilde{c}) \cong \frac{\partial}{\partial b}\left(\frac{m_s}{m_b}\, h\, D_b\, \frac{\partial \tilde{c}}{\partial b}\right) \quad . \tag{5}$$

An additional advantage is that the boundary condition (zero mass transfer) along the bankline is simpler to formulate.

The mass streamline and the equations thereof

Considering the formal similarity between the continuity equation of flow

$$\text{div } (h\, \underline{\tilde{v}}) = 0$$

and Eq.(1) it appears logical to trace the streamlines of the vector field $\underline{\tilde{J}}$ (these will be termed mass streamlines) and the expressions thereof corresponding to Eqs. (3) and (4). Adopting a similar approach (Fig.2) the first equation of the mass streamline becomes ($\tilde{J}_x \neq 0$):

$$\frac{dy}{dx} = \frac{m_x}{m_y} \frac{\tilde{J}_y}{\tilde{J}_x} = \frac{m_x}{m_y} \cdot \tan\alpha \tag{7}$$

where $\tilde{J}_x \cong \tilde{v}_x \tilde{c}$; $\tilde{J}_y = \tilde{v}_y \tilde{c} - \frac{1}{m_y} D_y \frac{\partial \tilde{c}}{\partial y}$.

In terms of the latter the tangent of the angle is given as

$$\tan\alpha = \frac{\tilde{v}_y}{\tilde{v}_x} - \frac{D_y}{m_y \tilde{v}_x \tilde{c}} \frac{\partial \tilde{c}}{\partial y} = \tan\alpha_q - \frac{D_y}{m_y \tilde{v}_x \tilde{c}} \frac{\partial \tilde{c}}{\partial y}. \tag{8}$$

The second equation, just as the condition dq = 0 is an expression of the fact that the mass transport perpendicular to the streamline (averaged again over time and depth) is zero:

$$d\dot{m} = 0 \tag{9}$$

where

$$\dot{m} = \int_{y_l}^{y} m_y \, h \, \tilde{v}_x \tilde{c} \, dy' \tag{10}$$

in terms of which the second equation becomes ($\partial\dot{m}/\partial y \neq 0$):

$$\frac{dy}{dx} = -\frac{\partial \dot{m}/\partial x}{\partial \dot{m}/\partial y} = -\frac{1}{m_y h \tilde{v}_x \tilde{c}} \frac{\partial}{\partial x} \int_{y_l}^{y} m_y \, h \, \tilde{v}_x \tilde{c} \, dy'. \tag{11}$$

In this way we have succeeded in describing the mass streamline by two equations, which are suited to determining the concentration field and the mass streamlines simultaneously. The solution of the problem is thus equivalent to the solution of Eq.(2).

The difference between the two sets of streamlines is readily appreciated from Eq.(8) and Fig.2. The angle α is composed of two parts, the first of which, α_q is the angle included by the vector $\tilde{\underline{v}}$ and the coordinate line, and is characteristic of the flow. The second, α_m is the spreading angle, which varies from point to point (it can be demonstrated to be always less than 90 deg.) and is determined by the mixing process taking place in the flow.

In the (s,b) system of coordinates $\tan \alpha_q = 0$ and the expressions assume the following simplified forms

$$\tan \alpha_m = - \frac{D_b}{m_b \tilde{v}_s \tilde{c}} \frac{\partial \tilde{c}}{\partial b} = - \frac{D_b}{m_b \tilde{v}_s} \frac{\partial}{\partial b} (\ln \tilde{c}) \tag{12}$$

$$\dot{m} = \int_0^b m_b h \tilde{v}_s \tilde{c} \, db' . \tag{13}$$

Evidently, Eqs, (7) and (11) are modified accordingly and similar simplifications become possible also by introducing the cumulative discharge.

<u>Boundary conditions</u>

There is no mass transfer across the banks

$$\frac{\partial \tilde{c}}{\partial b}(o) = \frac{\partial \tilde{c}}{\partial b}(B) = 0 \tag{14}$$

whence on the basis of Eq.(12)

$$\tan \alpha_m(0) = \tan \alpha_m(B) = 0. \tag{15}$$

On the upstream side of the section

$$\tilde{c}(0,b) = f_1(b) \tag{16}$$

is given, to which the condition

$$\tan \alpha_m(0,b) = f_2(b) \tag{17}$$

corresponds.

Properties of the mass streamline and the mixing process

The tangent of the spreading angle α_m according to Eq.(12) is proportionate to the product $D_b \partial \tilde{c}/\partial b$ (with an opposite sign). The wider the angle α_m, the more intensive is mixing. The contours of a plume starting from a polluting discharge (Fig.3) are bounded by streamlines. In the immediate vicinity of the discharge point (the source) the mass streamlines are parabolic in form described by $k\ s^{1/2}$, since here the change in concentration can be approximated by a simple Gaussian distribution.

The extreme streamlines approach gradually the banks and even adhere to these, as expressed by Eqs. (14) and (15). Hereafter the banks become not only streamlines, but also mass streamlines. Since the mass flux between two adjacent mass streamlines, thus in a mass flux tube remains always constant, the longitudinal change in concentration is due to a change in the flow rate within the mass flux tube (see later). Approaching uniform conditions $\partial \breve{c} / \partial b \longrightarrow 0$, so that $\alpha_m \longrightarrow 0$ and the mass streamlines tend to the streamlines (Fig.3).

COMPUTATION OF THE CONCENTRATION FIELD AND THE MASS STREAMLINES

Solution scheme

Consider the curved edge of the river section examined assuming the (s,b) system of coordinates, as well as all quantities involved in the solution to be available as functions of s and b. Using the method of finite differences the transverse trajectory s = 0 (j = 0) has only been subdivided into equidistant discrete elements along the definition domain of the function $\breve{c}(0,b)$. The mass streamlines which emerge from the points indexed i resulting in this way have been determined as described before. The concentration values have been obtained at the mid-points k of the mass flux tubes formed by the adjacent mass streamlines. The longitudinal increment Δs_j is not necessarily a constant one, it may be fixed in advance, or varied by steps on the basis of the stability condition (see Eq.(20)).

In general, the approximations to the mass streamlines are computed first between the trajectories j and (j+1) within the section Δs_j (Fig.4). For this purpose the value of $(\tan\alpha_m)_{i,j}$ is found by approximating ln $\tilde{c}$ with a Newton--Gregory polynom of second order. If no more than the values of the j-th level are included here, the arch-length $\Delta b(s^*)$ (Fig.4) will become within Δs_j a linear function of s^* : $\Delta b(s^*) = s^*(\tan\alpha_m)_{i,j}$ and the scheme obtained is an explicit one. Using instead of $(\tan\alpha_m)_{i,j}$ the value $[(\tan\alpha_m)_{i,j} + (\tan\alpha_m)_{i,j+1}]/2$ including the level (j+1), the term $\Delta b(s^*)$ will be of the second order and the method becomes an implicit one (this involves substantially no more than the application of the Crank-Nicholson formula).

Once the j and (j+1) approximations to the mass flux tubes have been determined, the term $\tilde{c}_{k,j+1}$ is found from a simple mass balance expression (Fig.4 and see also Eqs.(9), (11) and (13)):

$$\dot{M}_k \cong (h\,\tilde{v}_s\tilde{c}\,\Delta b)_{k,j} \cong (h\,\tilde{v}_s\tilde{c}\,\Delta b)_{k,j+1} \qquad (18)$$

whence $\tilde{c}_{k,j+1}$ is expressed for instance in the form

$$\tilde{c}_{k,j+1} = \frac{\Delta q_{k,j}}{\Delta q_{k,j+1}}\,\tilde{c}_{k,j} \quad . \qquad (19)$$

The foregoing line of reasoning leads, owing to Eq.(12), to a non-linear difference scheme. In the implicit method this is approximately one of second order in both directions, whereas of the first order longitudinally in the explicit method. As a consequence of non-linearity the former can be applied by successive approximation only.

Boundary conditions

The boundary condition $\tilde{c}(0,b)$ is assumed to be available from a near-field solution, or from measurement. Where this is not the case and a point source is considered, the condition $\tilde{c}(0,b)$ can be obtained from an analytical solution of Eq.(5) for the immediate surroundings of the source (in which range the coefficients may be considered virtually constant).

Up to the point where the plume reaches the bank, the extreme mass treamlines are found by including the first, or last three points. After the water edge is reached, the boundary conditions (14), (15) are satisfied with the help of reflected points.

Stability

Non-linearity of the method derived makes the conventional stability tests inapplicable. For this reason the equations of the explicit procedure have been linearized first then the norms of the errors in concentration and space coordinates estimated (with allowance to the interrelations between the two kinds of error) for different conditions $\tilde{c}(0,b)$ by determining the significant matrix norms. The investigations performed and the experiences gained in computation have shown for the method weak stability if the condition

$$\left(\frac{D_b \, \Delta s}{\tilde{v}_s \, \Delta b^2}\right)_{i,j} \leq 1 \qquad (20)$$

is satisfied (in steady problems stability of this kind is alone possible).

Computer programme

Two alternative programmes have been written in FORTRAN IV language. All relevant quantities and coefficients are needed to use the first. The second has been compiled for practical applications using the data normally observed in the hydrographic network and the information usually available. Thus for instance the determination of points of the water edge, mean velocities and depth distributions is based on the computation of surface profiles for particular streamflow rates, D_b is found from the expression $D_b = d\ Hu^{*}$, while the influence of bends is estimated from Fischer's (3) correlation. For determining the distributions $\tilde{v}_s(b)$ observation results, or the use of empirical formulae are needed.

This kind of programme enables us to examine approximately longer river sections (at different streamflow rates) even in cases, where no special observations can be performed.

Comparison of analytical and numerical solutions

For the partial verification of the method developed comparative tests have been performed by varying the main characteristics (D_b, $\tilde{v}_s$, Δs, Δb) for less complicated cases, where an analytical solution is possible (constant coefficients, different $\tilde{c}(0,b)$ conditions: point source at different distances from the water edge, parabola of the third degree, etc.). The results agreed very well (see Somlyódy (16)). The implicit method was found to be slightly more accurate, but because of the longer computer time, the use of the explicit method is suggested instead for practical purposes, and the latter has been adopted in each of the following examples.

Main features of the numerical method

The common feature of the familiar difference methods is that the number of points at which the concentration is other than zero tends to increase together with the value of j. Thus in the vicinity of a point source, where $\partial \tilde{c}/\partial b$ is high, a few points are only considered, the number of significant points increasing as the distribution becomes more uniform. Moreover, the edge of the plume depends greatly on the type of discretization adopted.

In the present method, as in the flow tube approach, the grid is in general non-uniform and the concentrations are obtained at the centres of the mass flux tube, rather than of the stream tube. The number of points included in the calculation is equal along each s = const. line. The results yields approximations of the mass streamline conforming to the physical particulars.

The detailed investigations related to the method presented here have been described earlier (16).

SOLUTION OF THE INVERSE PROBLEM: CALCULATION OF D_b

The aim here is to find the unknown $D_b(s,b)$ coefficient by applying the equations presented before to the case where the concentration field is also known (mostly from tracer measurements) along with the other quantities.

As the first step the distributions $\dot{m}(b)$ are determined in the cross-sections of observation. Hereafter $\tan\alpha_m(b)$ is found either from Eq.(9), or from Eq.(11), using the adjacent upstream and downstream cross-sections (see 15)). Two alternative paths can then be followed for determining D_b.

i) $D_b(s,b) = D_b(s)$

The first two terms of the series of Eqs.(12) are adopted as the starting basis. Both are multiplied by $h(b-b_1)$ and after rearrangement of terms the expression is integrated between the two edges b_l and b_r of the plume. From the resulting expression $D_b(s)$ is obtained in the form

$$D_b(s) = -\frac{1}{f(s)}\,\frac{1}{\dot{M}}\int_{b_l}^{b_r} m_s h\,\tilde{v}_s\tilde{c}\,\tan\alpha_m(b-b_1)db. \qquad (21)$$

Here b_1 refers to an arbitrary coordinate line, $\dot{M} = \dot{m}(b_r) = \dot{m}(B)$, while $f(s)$ is given as

$$f(s) = \frac{1}{\dot{M}}\left\{\left[\frac{m_s}{m_b}h\,c(b-b_1)\right]_{b_l}^{b_r} - \int_{b_l}^{b_r}\tilde{c}\,\frac{m_s}{m_b}h+(b-b_1)\frac{\partial}{\partial b}\left(\frac{m_s}{m_b}h\right)db\right\}. \qquad (22)$$

According to Eq.(21), D_b is proportionate to the first moment of the distribution $m_s h\,\tilde{v}_s\tilde{c}\,\tan\alpha_m$, and the latter being determined by the same $f(s)$ function that is involved also in the method of moments, if the latter is generalized to the (s,b) curvilinear system of coordinates (16):

$$D_b = -\frac{1}{2f(s)}\,\frac{d\sigma_b^2}{ds}\ . \qquad (23)$$

This reflects at the same time the correlation between the longitudinal change of the second moment σ_b^2 of the distribution $m_b h\,\tilde{v}_s\tilde{c}$ and the first moment of the distribution involved in Eq.(21) and containing also the $\tan\alpha_m$ term.

ii) $D_b(s,b)$

In this case the solution is obtained by numerical integration of Eq.(22) at s = const. Thus for instance, by applying the trapeze rule, the dispersion coefficient pertaining to the mid-points indexed k of the sections of width $\Delta b = (b_r - b_l)/N$ is found from the expression

$$D_{b_{k,j}} = \frac{\breve{v}_s(\tan\alpha_m)_{k,j}}{\ln\frac{\breve{c}_{i,j}}{\breve{c}_{i+1,j}}}\Delta b \qquad (24)$$

where Δb denotes now the actual arch length, while i refers to the points of the mass streamline.

To check the two solutions outlined in the foregoing, concentration distributions obtained analytically for assumed D_b values have been adopted as measurement results, using then the methods for calculating the D_b values considered to be unknown in this step. The results obtained by Eqs. (21) and (24) have then been compared with the starting values. The examination has shown the advisability of selecting the coordinates b_l, b_r in a manner that approximately 5 % of $(\breve{c}_{max})_j$ should pertain to these. At very low concentrations the computation of $\tan\alpha_m$ is rather uncertain. Otherwise the agreement was a very good one.

Of the two methods the second is more general, but also more sensitive to errors of measurement and evaluation. For this reason some smoothing technique is advisable when using Eq.(24). The first method is essentially equivalent with the generalized change of moment method - though slightly more complicated. In the latter the role of errors in the extreme concentrations may be a pronounced one owing to the presence of the factor $(b-b_1)^2$, on the other hand the determination of the derivative $d\sigma_b^2/ds$ is often inaccurate, especially where $\sigma_b^2(s)$ is highly non-linear. The relative influences of hydraulic effects and errors of measurement and evaluation on the changes of $\sigma_b^2(s)$ are in general difficult to determine. Similar difficulties arise in all methods (see also (2) and (6)), so that great care must be exercised when solving the inverse problem.

COMPARISON OF NUMERICAL AND OBSERVATION RESULTS

To study the process of mixing and to verify the methods developed, tracer measurements have been carried out on different streams comparing the numerical results with those observed. The results obtained by Holley (4) at the Delft Hydraulics Laboratory on the 1:50 undistorted physical model of the Ijssel river have also been included in the comparison. The investigations comprised thus the following cases:

A. Laboratory studies

A1. Open, straight rectangular flume in which the bottom roughness and injection point were varied ($Q = 0.05\ m^3s^{-1}$, $B = 1\ m$, $H = 0.13 \div 0.15\ m$, $S = 1 \div 5.10^{-4}$, length of measuring section $L = 12\ m$).

A2. Model of a slightly curved section of the Ijssel river. The channel is irregular (arrangement without groins). Injection at the centreline and at the side ($Q = 0.0141$ m^3s^{-1}, $B = 1.3 - 1.5$ m, $H = 0.08 - 0.09$ m, $S = 6.10^{-5}$, $L = 20$ m).

A3. Open, strongly curved rectangular flume with different injection points ($Q = 0.025$ m^3s^{-1}, $B = 0.5$ m, $H = 0.14$ m, $R/B = 1.71$, $S = 10^{-3}$, $L = 10$ m).

B. Field observations

B1. Kis-Rába, mildly curved, almost trapezoidal, lined irrigation canal, injection point close to the bankline ($Q = 8$ m^3s^{-1}, $B = 8 - 11.5$ m, $H = 0.95 - 1.17$ m, $R/B = 12-15$, $S = 4.1.10^{-4}$, $L = 250$ m).

B2. Danube stretch upstream of Budapest, between River Stations 1707 and 1660 km (investigations in two consecutive years at different sections, $Q = 1000-2000$ m^3s^{-1}, $B = 350-$ -500 m, $H = 3-5$ m, $S = 6 - 8.10^{-5}$).

B3. Rába river (tributary to the Danube). Meandering section, irregular channel, injection in the vicinity of the bank ($Q = 5.3$ m^3s^{-1}, $B = 18-28$ m, $H = 0.4-1.3$ m, $R/B = 5$, $S = 6.10^{-4}$).

The tracers used included dye solutions (Rhodamine B, methylene blue, Na-Fluoresceine) and occasionally a solution of sodium chloride. The tracer was injected as a point-, or vertical line source at a steady rate, virtually at the same velocity as that of the ambient flow.

The concentration was measured at 7 to 10 verticals in each cross section and at 3-5 points in each vertical. The results were then averaged over depth, the values normalized in the knowledge of the tracer flux $\dot{M}$ measured independently, in accordance with the continuity condition. During the field experiments discrete samples were taken for determining the concentration field and these were then analysed (the sampling times had been determined by previous tests for correct averaging). Under laboratory conditions a continuous conductivity meter of original design, connected to a punched-tape memory unit and a fibre-optic photometer were also used. Velocities were measured by means of a Delft current meter, which could also be connected to the memory unit and averaged pulses over periods from 0.1 to 60 seconds.

For evaluating the measurement data and for comparing them with the analytical results, the coefficient D_b was always determined first, using Eqs.(20) - (24), then the concentration field using the numerical method outlined before. (Thus rather than estimating D_b and $\tilde{c}$ simultaneously, as frequently practiced in the literature, two independent methods have been adopted.) Some of the results will be presented subsequently.

A.1 Open, straight, rectangular laboratory flume

The flume bottom consisted of 12 mm mean size sharp-edged gravel. The velocity distribution in the flume was rather non-uniform (Fig.6), probably due to the shortness of the inlet section. Owing also to this circumstance, the standard deviation of longitudinal velocity (mean value in the cross-section) increased in the direction of flow (see also Fig.5). The measurements have shown the transverse velocity components to be negligibly small.

Three of the concentration distributions pertaining to each of the central- and side, vertical line injections are illustrated in Fig.6. (In all examples shown the tracer used was a dye solution.) The curves are of a Gaussian character, although the dispersion coefficient D_b was not constant longitudinally, but displayed an increasing trend parallel to the variation of $\sqrt{\overline{v_s'^2}}$ (Fig.5). For injection along the bank the D_b values were consistently higher ($d = D_b/Hu^*$ was 0.08 and 0.12). D_b was calculated from Eqs. (21) and (23) alike, showing in Fig.5 also the uncertainty resulting from the formation of the derivative $d\vec{\sigma}_b^2/ds$.

The concentration field was calculated by adopting $N = 7$ mass flux tubes, with the condition $\check{c}(0,b)$ derived consistently from the analytical solution applying to the close vicinity of the source. The agreement with the observed values was always a very good one (Fig.6).

A.2 The Ijssel model

The arrangement of the model, the cross-sections of measurement, typical velocity- and depth distributions, further the plume contours pertaining to two different injection modes are shown in Fig.7. The results observed, and calculated by the method described, as well as those obtained by Verboom (19) for injection at the centerline have been compared in a previous paper (18).

The concentration distributions observed for injection at the bank are shown in Fig.8. (These have been normalized for a tracer flux $\dot{M} = 0.005$ C.U.$m^3 s^{-1}$, 1 concentration unit (C.U.) = $4.6.10^{-8}$ kg m^{-3}, see (4)). The evaluation has been based on the investigations of Holley, who has determined the dispersion coefficient among others under the assumptions $D_b(s,b)$ = const. and $D_b(s,b) = k\ h\ \tilde{v}_s$, calculating therefrom the concentration field. The agreement between the calculated and observed values in the 10-15 cm wide range along the bank was unsatisfactory in each case, as illustrated also by the results shown for cross-section No.2 in the figure. Holley has attributed this fact first of all to the transverse variations of D_b, the character of which is not described correctly by the expression $k\ h\ \tilde{v}_s$ (see Fig. 8). Moreover, the results seem to imply non-conservative properties of the numerical method applied (Fig.8).

In the present investigations $D_b(s,b)$ has been determined from Eq.(24), imposing no restriction whatsoever concerning the shape of $D_b(s,b)$. The result for cross-section No.2 has also been entered as an example in Fig.8. The functions $D_b(b)$ obtained have hereafter resulted in very good agreement between the observed and calculated concentrations (Fig.8, $N = 7$, $\Delta s = 1$ m).

B.1 The Kis-Rába river

The experimental stretch, the point of injection and the mass streamlines calculated ($N = 5$, $\Delta s = 12.5$-50 m) are shown in Fig.9. The typical velocity- and depth distributions in the first few cross-sections are shown in Fig. 10. The tracer was injected as a point source and became uniform over depth within 50 m. The concentration distributions obtained by measurement are shown in Fig.11. For the coefficient D_b the value 0.011 m^2s^{-1} ($d \cong 0.16$) has been obtained from Eqs. (21) and (23) alike, again with good agreement between the observed and calculated concentrations. The role of the velocity field should, however, be emphasized here. For instance, unless the distribution $\tilde{v}_s(b)$ in cross-section No.1 is known (Fig.10), it must be interpolated between the adjacent upstream and downstream cross-sections. As a consequence thereof, the approximations to the streamlines will be inaccurate and the concentrations calculated will differ strongly from the observed values.

B.2 The Danube

The experiment has been carried out upstream of Budapest, in the Vác Branch of the Danube, over a practically straight river stretch, in the vicinity of the right-hand bank. (For details see (15) - (17).) In the range of the plume, the calculated shape of which is shown in Fig. 12, the water depth ranged from 2-3 m, the flow velocity from 0.65 to 0.80 ms^{-1}, while the standard deviations of velocity from 0.04 to 0.09 ms^{-1}. The tracer was injected as a point source at mid-depth, and became uniform over depth practically within 100 m distance. Concentrations were measured in six cross-sections situated within a distance of 800 m (Fig.12). The dispersion coefficient found from Eq.(21) increased up to 600 m, whereafter it diminished again (Fig.12, $D_b(s)$), with $d \cong 0.25$ corresponding to the mean value of 0.038 m^2s^{-1}.

The longitudinal variations of highest concentration are shown in Fig. 13. When using $D_b(s)$ the agreement between the observed and theoretical values ($N = 8$, $\Delta s = 20$ m), as well as that of the transverse distributions (see (17)) is a very good one. The agreement is less satisfactory when using the mean value of D_b in the calculation (Fig.13), and to illustrate the sensitivity of the solution the results pertaining to D_b coefficients increased and reduced by 50 per cent have also been entered.

Evidently, the accuracy of the coordinates calculated is also of considerable importance, as illustrated in Fig.12 by the points of peak concentration observed. These depart in the last two cross-sections from the calculated location, in that $\tilde{c}_{max}$ is observable along the central mass streamline practically over the entire length. The difference is due to the sudden change in the river bed around 500 m from the source round 100 m from the bank-line, the influence of which is not reflected truly by the streamlines calculated from the velocity distributions. (The error in direction is slightly less than 7 degrees.)

The application of the mixing model presented, in combination with surface profile calculation (see before) over a round 60 km long stretch of the Danube has been described elsewhere (17).

LIMITATIONS TO THE TWO-DIMENSIONAL APPROACH.

THE DISPERSION COEFFICIENT

Consider first the series of equations defining the dispersion coefficient introduced after integration over depth:

$$\frac{1}{h} \int_{o}^{h} (\overline{c'v'_b} + \bar{c}^{*} \bar{v}_b^{*})\, dz = - \frac{1}{m_b} D_{bt} \frac{\partial \tilde{\bar{c}}}{\partial b} + \widetilde{\bar{c}^{*} \bar{v}_b^{*}} =$$

$$= - \frac{1}{m_b} (D_{bt} + \Delta D_b) \frac{\partial \tilde{\bar{c}}}{\partial b} = - \frac{1}{m_b} D_b \frac{\partial \tilde{\bar{c}}}{\partial b}, \qquad (25)$$

in which the asterik denotes the measured departures from the depth-integrated value. The first terms reflect the effect of turbulence, the second terms that of non-uniformities (mainly secondary currents) in the vertical. Both, and thus their sum, have been described by a Fick type law ($D_b = D_{bt} + \Delta D_b$).

Two different limiting factors will be considered subsequently, which result i) from the difficulties associated with the determination of the coefficients involved in the governing equation and ii) from the three-dimensional character of the phenomenon.

i) Let us examine a case where the introduction of a gradient-type transport is justified ($D_{bt} > 0$, $\Delta D_b \geq 0$). This is usually the case in alluvial channels if R/B > 5, and in the absence of sudden contractions or expansions. Under such conditions the correctness of the solution depends on the accuracy of $\tilde{v}_s(s,b)$ and $D_b(s,b)$. The influence of the former was illustrated by examples B.1 and B.2, whereas that of the latter by A.2 and B.2. Also, A.2 demonstrated the sensitivity of the solution to variations of D_b in the vicinity of the bank, where $\tilde{v}_s$ and h are also subjected to pronounced variations. For this reason $\tilde{v}_s(s,b)$ and $D_b(s,b)$ can only be estimated in practice. Field measurements are usually prohibitively expensive. The calculation of velocities for channel bands from calculated surface profiles (see for instance Holly (6)) is often unsatisfactory, while mean values for D_b can at the most be assumed instead of $D_b(s,b)$. As a consequence, no more than limited accuracy could be expected from the solution, so that interest has been concentrated on an overall description of mixing, on the determination of the principal characteristics (plume width, the average concentration related thereto, the mixing length, sensitivity, etc.).

ii) The second limitation results from the assumption under Eq.(25), and from the introduction of the concept of dispersion. The mathematical problem is substantially simplified thereby, but it is usually impossible to verify their validity. The transport $\overline{c^{*}\bar{v}_b^{*}}$ reflecting to three-dimensional effects may be of a kind differring from assumed one, amplifying in some parts of the flow ($D_b > D_{bt}$) and diminishing in other parts ($D_b < D_{bt}$) the effect of turbulence. In extreme cases D_b may even become negative (see (2) and (12)). Under such conditions, further where D_b fluctuates strongly in the plane, the two-dimensional approach is obviously inapplicable. Similar experiences have been made during the investigations A.3 and B.3. One of the results obtained in the experiments in the strongly curved laboratory flume is shown in Fig.14. Contrary to expectations, the peak velocities occurred along the inner, rather than the outer side of the curve. The secondary currents developing could clearly be traced by component measurement and resulted, logically, in considerable transverse slopes. From the concentration distributions observed it will be appreciated in agreement with the results of Chang (2) that the edge of the plume separates from the wall, the line of peak concentrations approaching the centerline of the flume. Assuming the validity of a Fick-type law, it is impossible to describe this behaviour in two dimensions. The dispersion coefficient varies depending on the amplifying or diminishing effect of secondary flow, the average over the full stretch being $d \cong 0.35$ according to Eq.(23) . Over the section 0-1 its value is small ($\Delta D_b < 0$), increasing thereafter substantially (section 1-3, $\Delta D_b \gg D_{bt}$, $d \cong 0.85$), turning negative between 3 and 4 ($\Delta D_b < 0$, $|\Delta D_b| > D_{bt}$), assuming eventually again a positive value ($d \cong 0.60$). Neither can the transverse changes be neglected. For instance, in cross-section 2,where a positive average was obtained by the method of moments, Eq.(25) yields $d \cong -0.08$ at 5 cm distance from the right-hand flume wall with the velocities, concentrations and pulsations measured.

In connection with the dispersion coefficients derived from the various tracer measurements, additional conclusions can be arrived at. Introducing also the results of the experiment B.3 ($d \cong 1.6$), the dimensionless dispersion coefficient related to width, $D_b/u^* B$, tends to decrease hyperbolically with increasing B/H ratios, in agreement with the results of Lau and Krishnappen (8) obtained in straight, rectangular flumes. This implies that the magnitude of D_b is strongly affected through ΔD_b by the secondary currents. Moreover, from investigations on a small stream Muszkalay (10) has demonstrated that in the modified relationship obtained by introducing Nikuradse's roughness into the expression $D_b = d\ Hu^*$, the fluctuation of the resulting dimensionless dispersion coefficient is substantially reduced. This implies the role of friction. Using the available and future data it is, therefore, considered logical to attempt a description of D_b by combining the parameters D_{bt}/Hu^* and $\Delta D_b/Bu^*$, which can be correlated separately with different hydraulic and geometric quantities.

The elimination of both kinds of limitations mentioned in this section can be expected from adopting the generalized approach referred to in the introduction. Adherence to the two-dimensional treatment is bound to fail in providing a solution for ΔD_b, as well as in resolving the second limitation even if the equations of motion and continuity, further the turbulence model are introduced. This can be expected from the three-dimensional approach alone.

SUMMARY AND CONCLUSIONS

The phenomenon of transverse mixing has been studied, by assuming steady conditions. The concept of the mass streamline has been introduced as the streamline of the mass density vector field. There is no transport perpendicular to this streamline. The mass streamline has been defined by two equations written preferably in a curvilinear system of coordinates consisting of the streamline and the trajectories perpendicular thereto. The mass streamlines and the concentration field have been determined simultaneously by the method of finite differences. The former present a visual picture of the mixing process. The expressions derived are suited also to calculating the transverse dispersion coefficient, if the concentration field is known. Two methods have been presented, the first resembling in character to the generalized method of moments, the second enabling also the determination of transverse variations of D_b.

With the aim of verifying the methods developed for determining the concentration field and the dispersion coefficient, the analytical and numerical solutions, as well as the theoretical and observed concentrations have been compared for different cases. Tracer measurements have been performed on five streams of different character (Q = 0.25--2000 m^3s^{-1}) and data published in the literature have also been included. The limitations of the two-dimensional approach have been analysed finally.

The main conclusions are as follows:

i) The investigations performed have demonstrated the methods derived on the basis of the mass streamline equation to be suited to calculating the concentration field and the transverse dispersion coefficient.

ii) In the absence of sudden changes in channel geometry, and of strong curvatures, there was satisfactory agreement between the theoretical and osberved values, supporting the applicability of the two-dimensional approach. However, the agreement depended in closeness on the accuracy with which the velocity field and the dispersion coefficient could be determined. Aside from the longitudinal-, the transverse variations of D_b had to be taken into account occasionally. These latter are especially important in the vicinity of banks. For determining the velocity field and the variable dispersion coefficient involved in the two-dimensional approach, no adequately supported method in thus far available. The dispersion model can thus be expected to yield results of limited accuracy alone, an overall description of the phenomenon being its primary merit.

iii) In the presence of sharp bends, expansions and contractions, the effect of turbulence on mixing is amplified or diminished by the secondary currents developing. The dispersion coefficient fluctuates accordingly in both directions considerably, assuming potentially even negative values.

In such cases a generalized, three-dimensional approach involving the equations of motion and continuity, further the turbulence model is alone likely to be successful. In this domain intensive research is considered desirable.

iv) In the experiments on the various streams the ratio B/H ranged from 3.5 to 100. Values from 0.08 to 1.6 have been obtained for the dimensionless dispersion coefficient D_b/u^*H. The coefficient D_b/u^*B related to width decreased hyperbolically with increasing B/H values, implying that D_b is influenced considerably by secondary currents. The role of friction is also an important one. It appears logical, therefore, to correlate the share of turbulence with the product Hu^*, that of irregularity over depth with the product Bu^* which, in turn, can be correlated individually with different geometric and hydraulic quantities. The dispersion coefficient is likely to result hereafter by some combination of the two terms.

APPENDIX I. - REFERENCES

(1) Bansal,M.K., "Dispersion in natural streams", Journal of the Hydraulics Division, ASCE, Vol.97. No.HY1. Proc. Paper 8540 November 1971, pp. 1867-1886.

(2) Chang,Y.C., "Lateral mixing in meandering channels" thesis presented in partial fulfillment of the requirements for the degree of Doctor of Philosophy, The University of Iowa, 1971, p.195.

(3) Fischer,H.B., "The effect of bends on dispersion in streams", Water Resources Research, Vol.5. No.2. April 1969, pp. 496-506.

(4) Holley,E.R., "Transverse mixing in rivers". Report of Delft Hydraulics Laboratory, S 132, 1971. p.92.

(5) Holley,E.R., Siemons,J. and Abraham,G., "Some aspects of analyzing transverse diffusion in rivers", Journal of Hydraulic Research 10 (1972) no.1., pp.27-57.

(6) Holly,F.M. Jr., "Two-dimensional mass dispersion in rivers", Hydrology Papers, Colorado State University, Fort Collins, Colorado, No.78. 1975, p.67.

(7) Krishnappen,B.G. and Lau,L.Y., "Transverse dispersion in meandering channels", Scientific Series No. 75, Inland Waters Directorate, Canada Centre for Inland Waters, Burlington, Ontario, 1977, p.98.

(8) Lau,L.Y. and Krishnappen,B.G., "Transverse dispersion in rectangular channels", Journal of the Hydraulics Division, ASCE, Vol.103, No.Hy 10, Proc.Paper 13294, October 1977, pp. 1173-1189.

(9) Launder,B.E. and Spalding,D.B., "The numerical calculation of turbulent flows", Computer methods in applied mechanics and engineering, Vol.3. 1974. pp.269-289.

(10) Muszkalay,L., "Determination of the relationship between the turbulent dispersion coefficients and mixing lengths" (in Hungarian). VITUKI Report, I.2.4.1. 1978, pp. 56.

(11) Paal,L.L., Velner,H.A., Liiv,U.R. and Rodziller,L.O., "The role of hydraulic factors in water quality control", Proc. of 15th Congress of the IAHR, Istanbul, 1973, B2.

(12) Sayre,W.W., "Natural mixing processes in rivers" in Environmental impact on rivers (River mechanics III), edited and published by Hsieh Wen Shen, Fort Collins, Colorado, 1973. Chapter 6.

(13) Sayre,W.W. and Chang,F.M., "A laboratory investigation of open-channel dispersion processes for dissolved, suspended and floating dispersants", U.S. Geological Survey Professional Paper 433-E, Government Printing Office, 1968, p.71.

(14) Somlyódy,L., "Examination of mixing in water streams using mass flux constant curves", Acta Technica, Tomus 82. (1-2), 1976. pp. 197-210.

(15) Somlyódy,L., "Dispersion measurement on the Danube", Water Research, Vol. 11. 1977, pp. 411-417.

(16) Somlyódy,L., "Determination of the effluent mixing process in streams by introducing the mass streamline

concept (in Hungarian). Thesis presented for the degree of Candidate of Science. Hungarian Academy of Science, Budapest, 1978. pp. 150.

(17) Somlyódy,L., "Mixing model for large streams", Progress in Water Technology, Vol.10. Nos. 5/6, pp. 97-104.

(18) Somlyódy,L., "The use and limitations of two-dimensional mixing model for rivers", IAHS-AISH Publ. No. 125. 1978, pp. 96-105.

(19) Verboom,G.K., "The advection-dispersion equation for an an-isotropic medium solved by fractional steps method", Delft Hydraulics Labaratory, Publ. no.157, 1975, p.14.

(20) Verboom,G.K. and Vreugdenhil,C.B., "Basic aspects of mathematical models", Proc. of european course on heat disposal from power generation in the water environment, Delft, 1975, Chapter 9.

(21) Yotsukara, N. and Cobb., E.D., "Transverse diffusion of solutes in natural streams", U.S. Geological Professional Paper 582-C, Government Printing Office, Washington, 1972, p.19.

(22) Yotsukara,N., Fischer,H.B. and Sayre,W.W., "Mixing characteristics of the Missouri River between Sioux City, Iowa and Plattsmouth, Nebraska", Water Supply Paper 1899-G, U.S. Geological Survey, Government Printing Office, Washington, 1970, p. 29.

(23) Yotsukara,M. and Sayre,W.W., "Transverse mixing in natural channels", Water Resource Research, Vol. 12. No.4. 1976. August, pp. 695-704.

APPENDIX II. - NOTATION

B	width
c	concentration
D_y, D_b	dispersion coefficients along y and b
d	dimensionless dispersion coefficient
$\underline{e}_x$, $\underline{e}_y$, $\underline{e}_s$, $\underline{e}_b$	unit vectors
h	local flow depth
H	hydraulic radius
$\underline{J}$	mass flux density vector
J_x, J_y, J_s, J_b	components of the mass flux density vector
i, j, k, N	integers
m_x, m_y, m_s, m_b	metric coefficients
$\dot{m}$	mass flux distribution
$\dot{M}$	mass flux
q	cumulative discharge
Q	streamflow
R	radius of curvature
S	surface slope
(s,b)	orthogonal, curvilinear set of coordinates consisting of streamlines and trajectories perpendicular thereto

u^*	shear velocity
$\underline{v}$	velocity vector
v_x, v_y, v_s, v_b	velocity components
(x,y)	orthogonal, curvilinear set of coordinates
α, α_m, α_q	characteristic angles of the velocity- and mass flux density vectors
σ_b^2	second moment
a	depth integrated value of quantity (a)
a^*	deviation of quantity (a) from a
$\underline{a}$	(a) vector

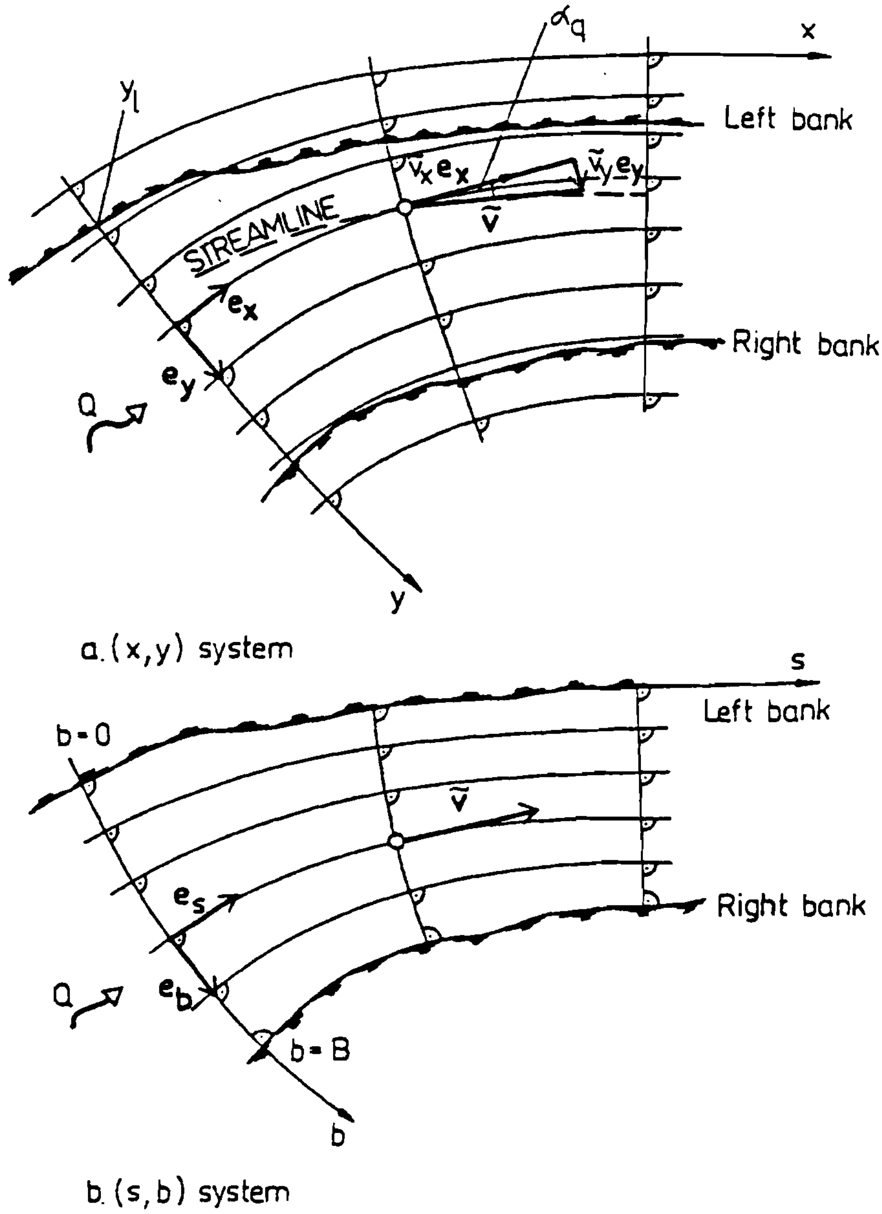

Fig.1. Orthogonal curvilienar coordinate systems

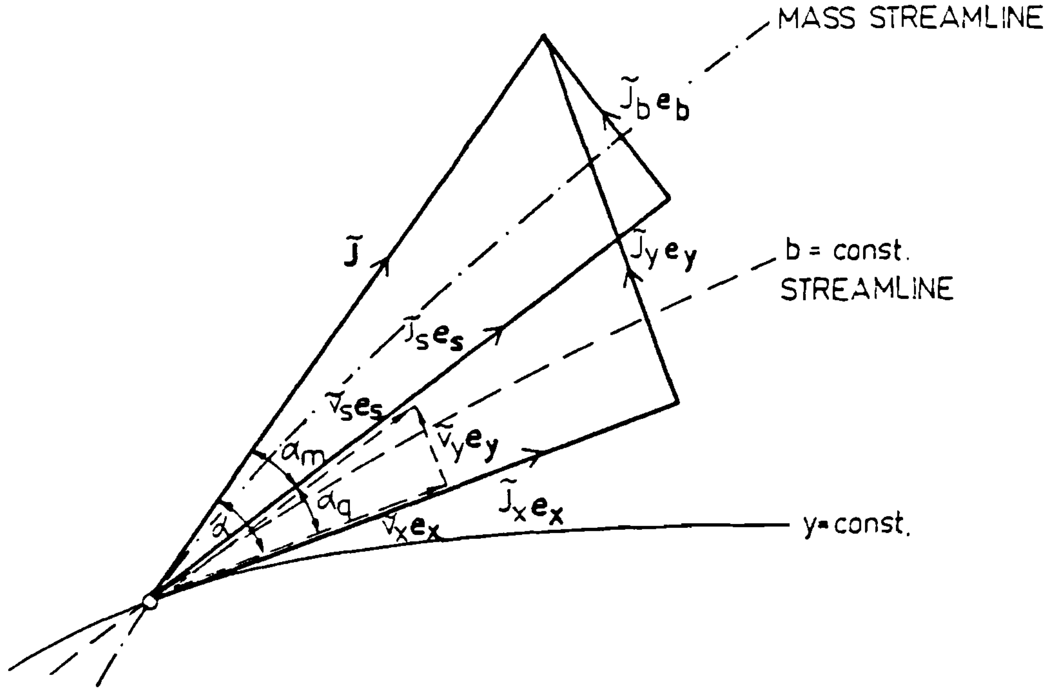

Fig .2. Definition sketch for the mass density vector in the (x, y) and the (s, b) coordinate systems

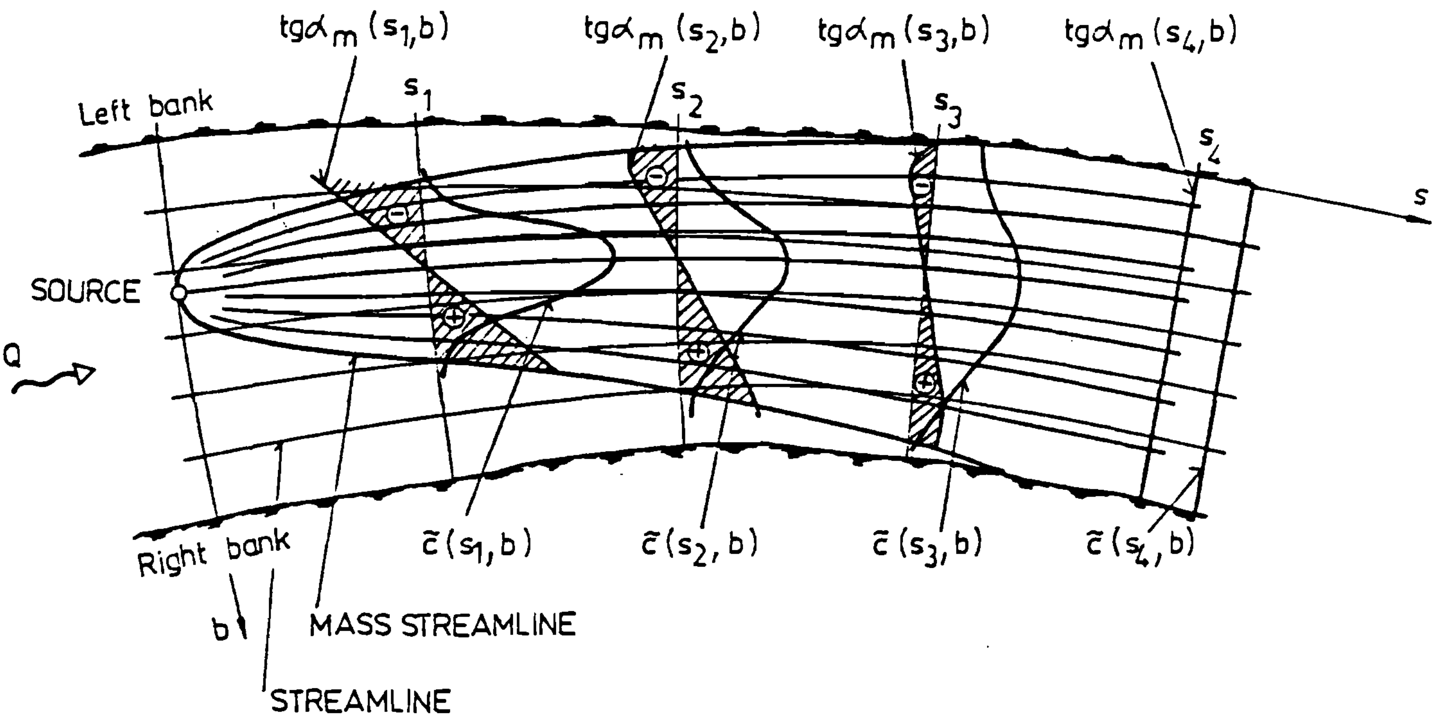

Fig. 3. Properties of mass streamlines and the mixing process

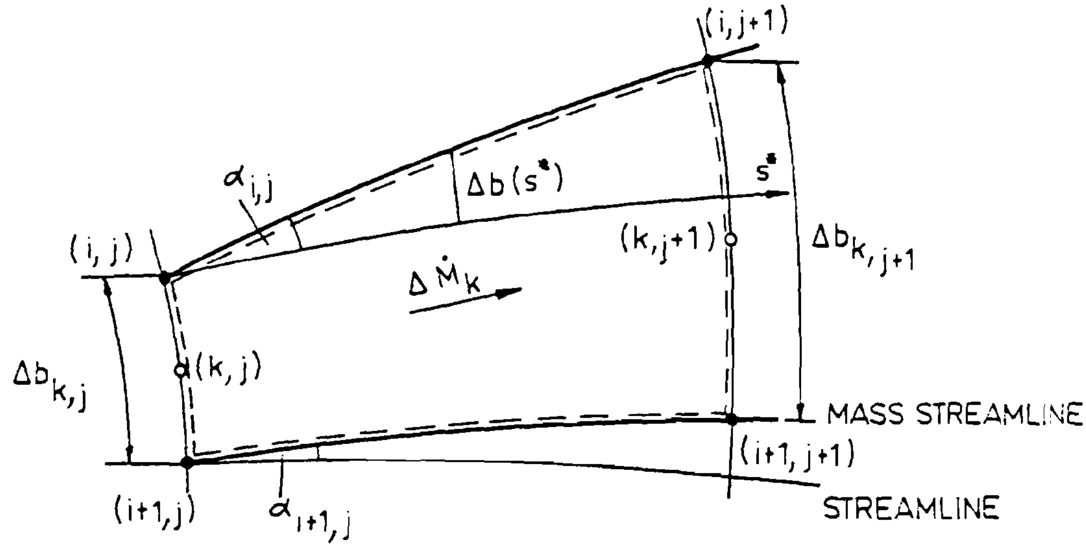

Fig. 4. Derivation of the numerical solution

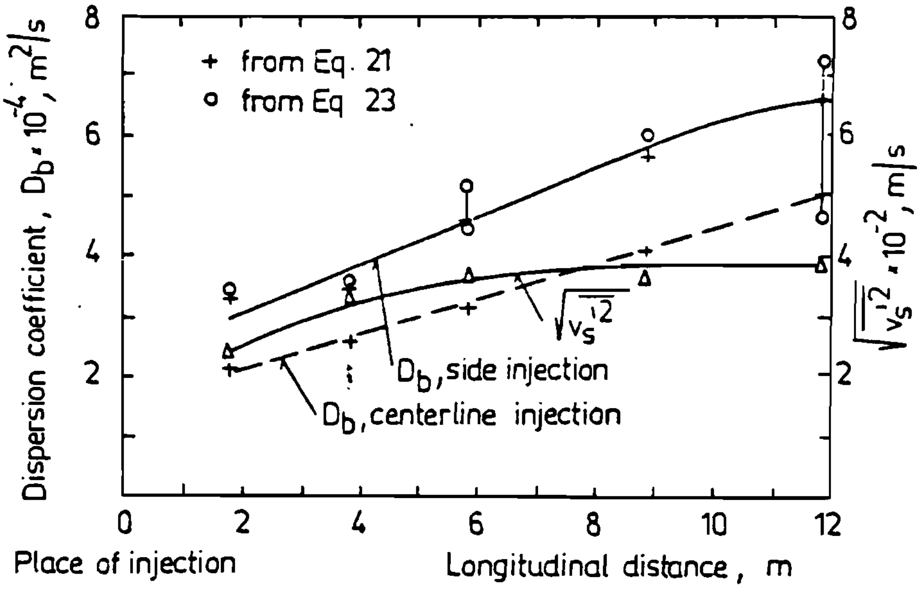

Fig. 5. Longitudinal variation of D_b and $\sqrt{\overline{v_s'^2}}$
Laboratory flume.

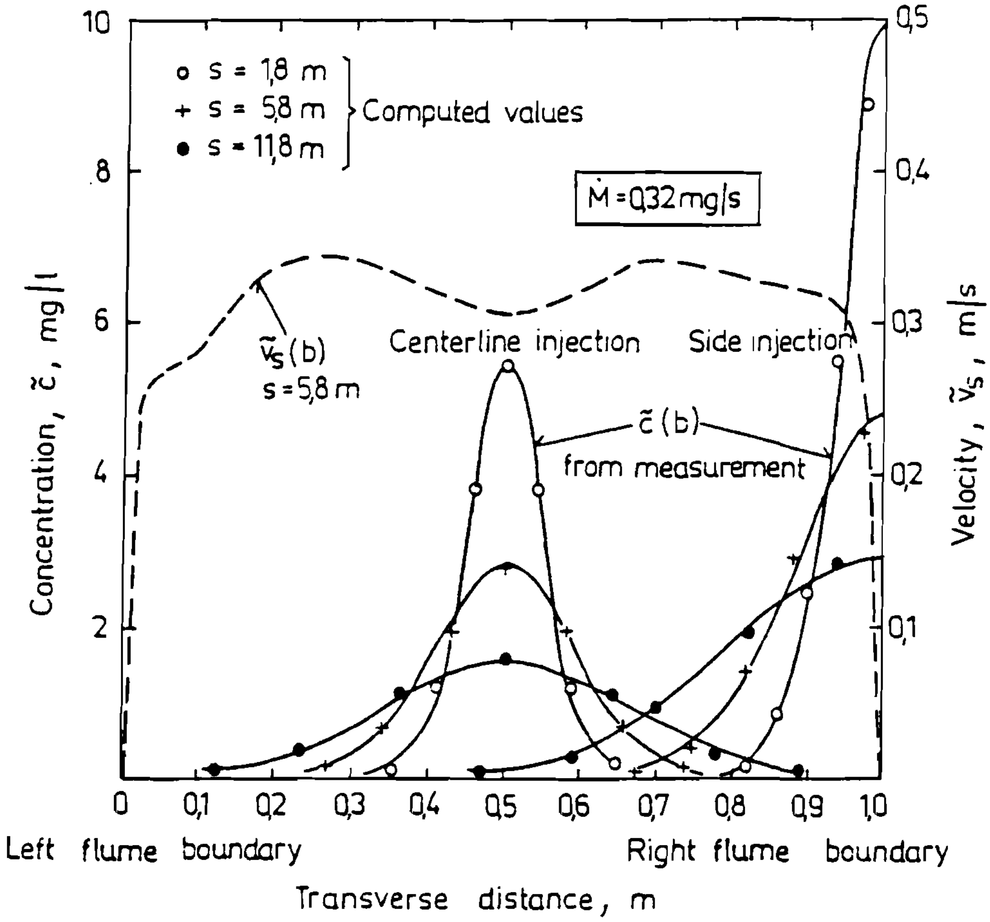

Fig. 6. Comparison of measured and computed concentrations. Laboratory flume.

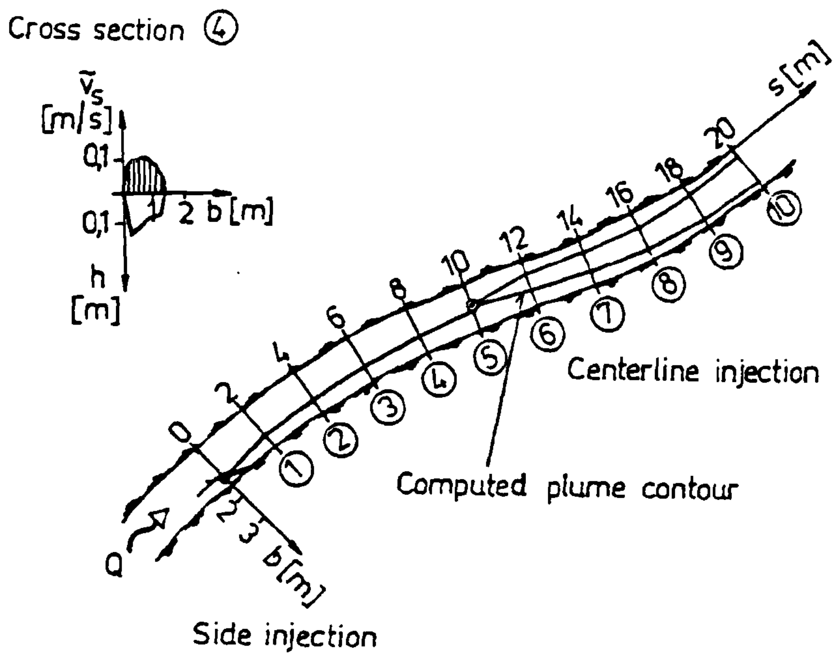

Fig.7. Layout of the Ijssel model

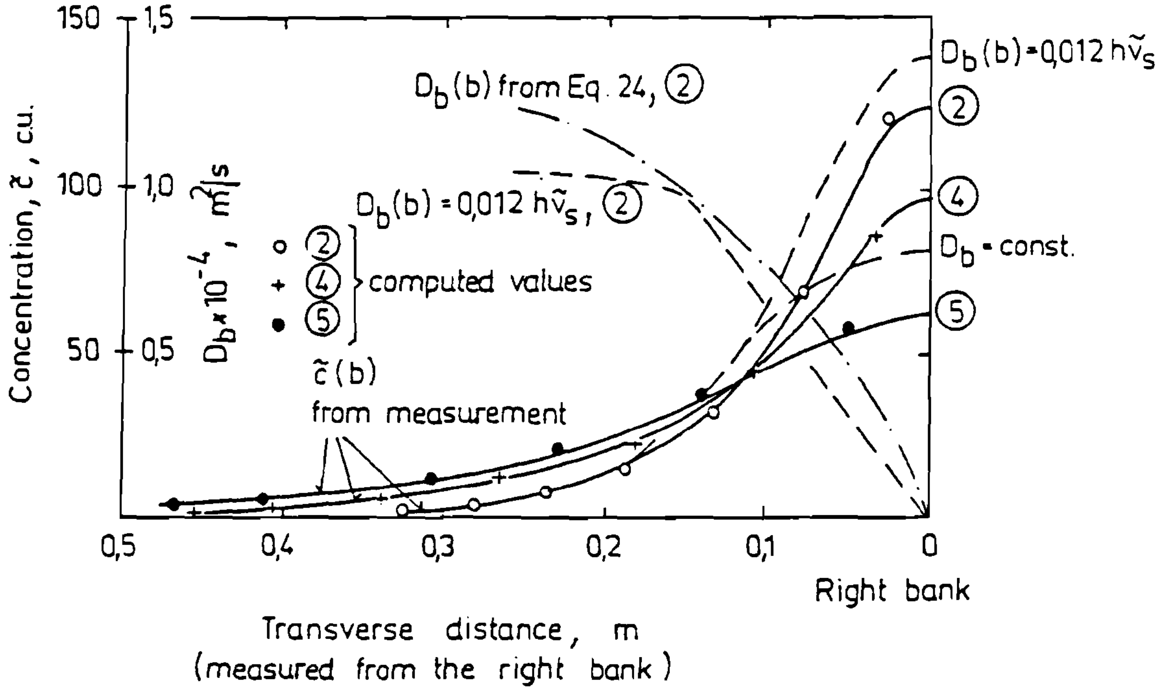

Fig. 8. Comparison of measured and computed concentration. Ijssel model, side injection.
---- computed by Holley (4).

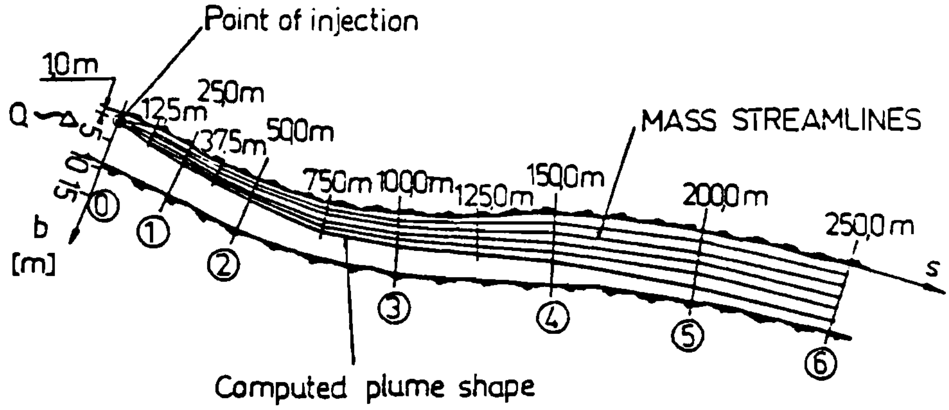

Fig. 9. Examined stretch of the Kis-Rába River.
The computed plume shape.

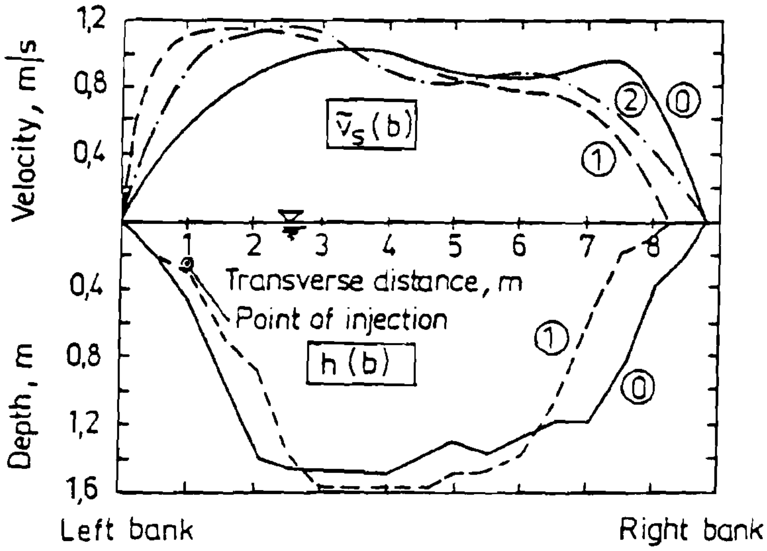

Fig. 10. Kis-Rába River. Velocity and depth conditions.

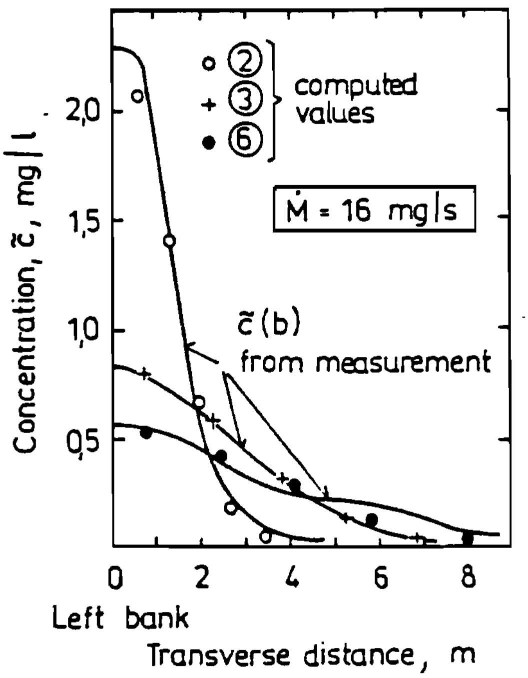

Fig.11. Comparison of observed and computed concentrations. Kis-Rába River.

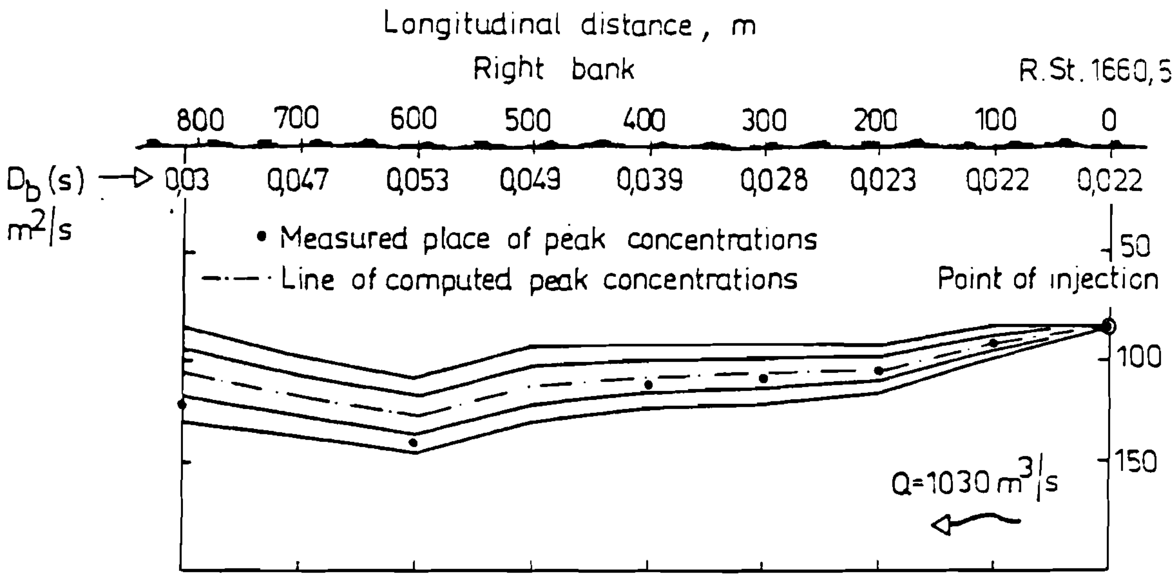

Fig.12. Computed plume shape. Danube River.

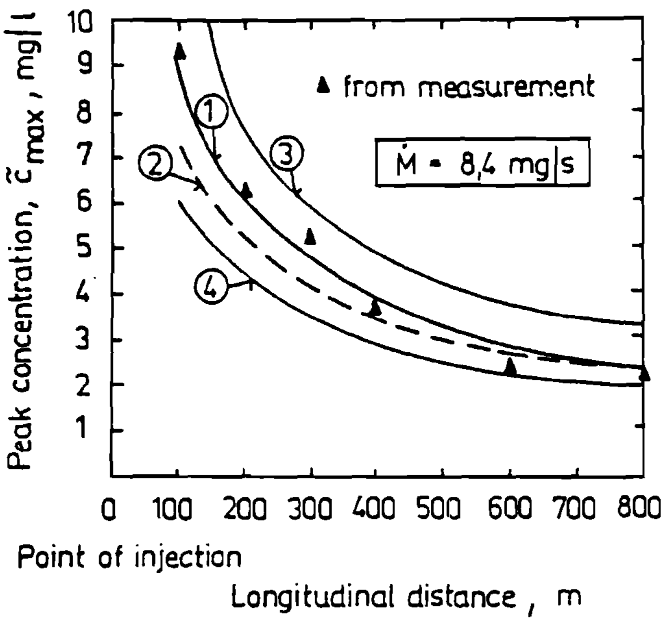

Fig.13. Comparison of observed and computed concentrations. Danube River

① $D_b = D_b(s)$ ② $D_b = 0{,}038\ m^2/s$

③ $D_b = 0{,}019\ m^2/s$ ④ $D_b = 0{,}057\ m^2/s$

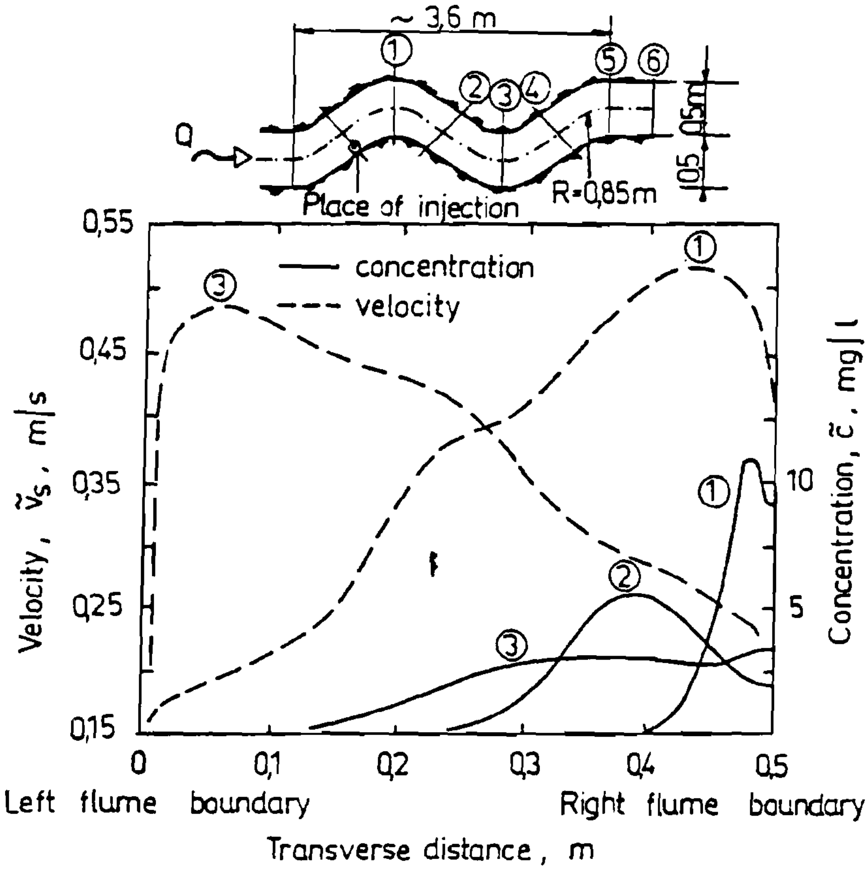

Fig.14. Measured concentrations and velocities. Curved laboratory flume.